

18th CIRP Conference on Intelligent Computation in Manufacturing Engineering

In-process measurement of vibrations in ultrasonic vibration superimposed turning using mechanical feedback signals

Jonas M. Werner^{a,*}, Hendrik Liborius^b, Welf-Guntram Drossel^{a,c}, Andreas Schubert^b

^aProfessorship for Adaptronics and Lightweight Design in Production, Chemnitz University of Technology, Reichenhainer Straße 70, 09126 Chemnitz, Germany

^bProfessorship Micromanufacturing Technology, Chemnitz University of Technology, Reichenhainer Straße 70, 09126 Chemnitz, Germany

^cFraunhofer Institute for Machine Tools and Forming Technology IWU, Reichenhainer Straße 88, 09126 Chemnitz, Germany

* Corresponding author. Tel.: +49-371-531-32203; fax: +49-371-531-832203. E-mail address: jonas-maximilian.werner@mb.tu-chemnitz.de

Abstract

Performance of components or systems can be significantly enhanced by surface microstructuring. Ultrasonic vibration superimposed turning is a highly efficient method for this, including the microstructuring in finish machining. However, control of these processes under varying loads is difficult and requires constant regulation of the systems operating frequency and vibration amplitude. Applying sensors to measure mechanical vibrations and using them to control the system offers benefits over conventional approaches like phase-locked-loop (PLL) or autoresonant control. In the experimental investigations, two sonotrodes are designed to integrate a variety of sensors for vibration measurement. Strain gauges, fiber-optical sensors, an accelerometer, and a passive piezoelectric disk in the ultrasonic transducer have been chosen. The performance of the sensors is examined for a free vibration as well as in an ultrasonic vibration superimposed turning process. The sensors are evaluated at different operating frequencies and power levels as well as varied loads during manufacturing resulting from different feeds (0.05 mm and 0.1 mm). Furthermore, the cutting speed is varied (120 m/min and 480 m/min) to change the rotational frequency of the spindle. Results show that all of the sensors prove useful in measuring the vibrations and determining the resonance frequency of the system during operation. The research improves understanding of the benefits of measuring different mechanical properties (strain, acceleration) in ultrasonic vibration superimposed turning, allowing for a more accurate in-process monitoring of the ultrasonic vibration and the control of the system in the future.

© 2025 The Authors. Published by Elsevier B.V.

This is an open access article under the CC BY-NC-ND license (<https://creativecommons.org/licenses/by-nc-nd/4.0>)

Peer-review under responsibility of the scientific committee of the 18th CIRP Conference on Intelligent Computation in Manufacturing Engineering (CIRP ICME '24)

Keywords: ultrasonics; process monitoring; vibration superimposed turning

1. Introduction

Growing standards for a higher precision in manufacturing require a continuous improvement of production processes. In this context, hybrid processes are becoming increasingly important. One group of those enhanced processes are ultrasonic vibration assisted manufacturing processes. Including ultrasonic vibrations in machining operations like turning or drilling [1] as well as in forming like wire drawing [2] or upsetting [3] can improve the performance markedly.

Benefits of an ultrasonic vibration assistance in machining can include, inter alia, an extension of the tool life, an improvement of chip breakage or a reduction of burr formation. Furthermore, machining of brittle materials like ceramics or glass is improved [4, 5, 6, 7, 8]. Reasons for this are diverse as the advantages themselves and strongly depend on the vibration direction. A shorter contact time between the tool and workpiece, and therefore a shorter diffusion process and decreased cutting forces on average, affect the process performance.

Ultrasonic vibration systems usually consist of a signal generator, an ultrasonic transducer, and a sonotrode [9, 10]. The generator supplies a voltage at the resonance frequency of the system to the transducer, often a piezoelectric stack, which converts the electrical signal into a mechanical vibration via the inverse piezoelectric effect. While transducers typically have the same general design, the sonotrode is designed with a specific application in mind as it affects the vibration shape and the amplitude of the system. For different processes the design of the sonotrode varies strongly [2, 11, 12, 13]. For turning processes, the cutting tool is placed at the front end of the sonotrode.

A typical application of ultrasonic vibration superimposed machining (UVM) is the microstructuring of surfaces directly in the finishing process [14, 15, 16, 17]. Changing loads during machining (thermal influences, load from the process itself) affect the dynamic properties of the ultrasonic system and may cause a shift of the resonance frequency. To produce defined microstructures with UVM, a system to control the vibration frequency and amplitude under changing loads is necessary. Using a fixed frequency is also possible, but involves reduced amplitudes.

Currently, control systems are based on electrical feedback signals from the transducer. Available electrical parameters like current, voltage, power, or phase shift are commonly used. Well known control systems are for example the phase-locked-loop (PLL) or autoresonant control, both aiming to keep the phase shift between the voltage and current at 0° [18]. Irrespective of the exact control system employed, the data acquisition is far away from the cutting process [19]. Due to the physical distance between the electrical parts and the cutting tool, the use of signals based on mechanical properties close to it offers benefits regarding the content of information of the current process behavior. By measuring the displacement or the acceleration during the process a more direct characterization of the in-process behavior is possible. In several investigations, this is analyzed, recommending mechanical parameters (displacement, strain, acceleration) for a possible control system [20, 21, 22, 23].

The permanent fixation of sensors under industrial standards or even the optical accessibility are limiting factors. Furthermore, requirements regarding the sampling rate of the sensors, their dimension and weight strongly reduce the amount of options available. Previous work regarding promising sensors have included strain gauges, accelerometers, and structurally integrated piezoceramics [20, 24]. If a suitable sensor for measuring vibrations of ultrasonic systems used for machining is found, it might enable the design of a more precise control system for UVM.

2. Experimental Design

2.1. Sensors

For the evaluations, a new research-specific system is designed. For selecting appropriate sensors, the behavior of ultrasonic systems has to be known. During vibration the

transducer and the sonotrode expand, contract and a standing wave occurs. Hence, the system exhibits zones of zero displacement and high strain (nodes) and zones of high displacement and zero strain (antinodes). The system itself is mounted at the nodes and the tool is placed at an antinode to realize a high displacement. This also influences reasonable sensor positions for different kinds of measurands. For the evaluations the following sensors have been chosen:

To compare the mechanical signals with an electrical signal, a passive piezoceramic disk is integrated into the transducer. While the other piezoceramic disks operate as an actuator using the inverse piezoelectric effect, the sensor disk, consisting of the material SONOX P8 (Ceramtec GmbH), utilizing the direct piezoelectric effect. The same ceramic material is chosen for the actuator disks (PZT-8). Changes to the dynamic properties of the ultrasonic system are minor since the integration of the additional piezoelectric disk has been taken into account during design.

Furthermore, an accelerometer is used to measure the vibrations. This enables a direct calculation of the displacement during the manufacturing process. Factors that have to be considered for the selection of a suitable accelerometer are the fixation, the routing of the cable, its weight, and limitations regarding the sampling rate and maximum frequency. According to the explanation given above, the accelerometer should be placed at an antinode, ideally close to the tool. For the experiments the accelerometer PCB 352A92 (PCB Synotech) is chosen. It is a uniaxial ICP (integrated circuit piezoelectric) accelerometer. The flat surface at the front end of the sonotrode is a suitable position for this sensor. For mounting the sensor a small pocket at this face is produced by milling. To reduce the influence of these modifications on the vibration shape of the ultrasonic system, the sensor is placed along the longitudinal axis of the sonotrode to decrease bending. The low weight of the sensor (0.16 g) only marginally influences the vibration behavior.

For measuring the strain of the sonotrode during operation two different kinds of strain sensors are used: Firstly, strain gauges of the LY series type 10/350 CLY47-3L-2M from HBM/HBK with a measurement grid of 10 mm by 5 mm, which are specifically chosen to match the thermal expansion coefficient of the sonotrode material. Previous work showed their suitability for measuring ultrasonic vibrations [24]. Due to the low weight, the dynamic properties of the system are not noticeably affected. This also enables flexible placement of the strain gauges along the longitudinal axis of the sonotrode. In accordance with the explanation given previously the strain gauges are placed close to the node where the strain reaches its maximum. As the system is mounted at the node, the strain gauges are placed as close as possible to the node. To get detailed information regarding the vibration shape during the process, four strain gauges are placed along the circumference of the sonotrode. Additionally, two strain gauges are mounted near the indexable insert to compare the suitability of the sensors at areas with lower strain.

Secondly, fiber-optical sensors are utilized, which include fiber bragg gratings (FBG) and therefore several sensors in a

single fiber. In the investigations a fiber with three sensors is used. Moreover, the requirements for the strain gauges are relevant for the fiber-optical sensors. The sensor itself is placed in a blind hole along the longitudinal axis of the ultrasonic system, fixed with epoxy resin. This way, only strain of the neutral fiber is measured. Two of the three engraved bragg gratings work as a strain sensor, while the third one acts as a temperature sensor. The fiber used is a SM 9/125 μ -PI fiber from INFAP GmbH with wavelengths ranging from 1310 nm – 1650 nm. The specific wavelengths of the gratings are 1544 nm for the first strain sensor, 1553 nm for the second strain sensor and 1564 nm for the temperature sensor.

2.2. Ultrasonic system

For the evaluations, a research-specific system is designed with the necessary alterations for the sensors in mind. As the installation space available with only one sonotrode is not sufficient for mounting the accelerometer as well as the fiber-optical sensor, two, otherwise identical, sonotrodes are used. The transducer consists of three piezoelectric disks (two active, one passive as described above) made of SONOX P8 sandwiched between two Ti6Al4V masses. A screw is used to preload the piezoelectric stack. The screw itself is insulated with a PTFE insert.

The strain gauges and the accelerometer are applied to the Sonotrode 1 (Fig. 1a), while Sonotrode 2 incorporates the fiber-optical sensor (Fig. 1b). The transducer and the sonotrode are shown in Fig. 1 and 2. The system is mounted at the flange of the sonotrode. To control the system an ultrasonic generator from Optel Z.o.o. is used.

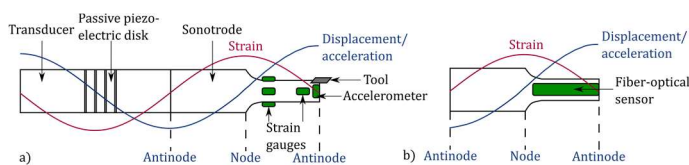


Fig. 1. Sensor arrangement
(a) Transducer with Sonotrode 1; (b) Sonotrode 2.

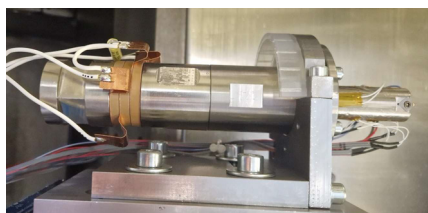


Fig. 2. Transducer and Sonotrode 1 with the strain gauges and the accelerometer.

3. Methodology and preliminary investigations

To characterize the behavior of the ultrasonic system and the sensors, the system has to be examined out of process to determine resonance frequencies and the corresponding

displacement. To achieve an in-depth insight into the dynamic properties of the system, the electrical as well as the mechanical vibration behavior were analyzed.

Firstly, an impedance analysis using an impedance analyzer (Zurich Instruments) of the system showed a resonance frequency for a longitudinal vibration of 22,845 Hz. The impedance curve and the phase response are given in Fig. 3a.

Secondly, the mechanical vibration behavior was analyzed using a 3D laser scanning vibrometer (PSV-500-3D, Polytec GmbH). A periodic chirp signal with an amplitude of 10 V was utilized as an excitation with a frequency up to 50,000 Hz. The resonance frequency for the longitudinal vibration is determined with 22,850 Hz, see Fig. 3b.

After this, the sensors themselves had to be evaluated out-of-process in the relevant frequency range. The experimental plan for this is given in Table 1.

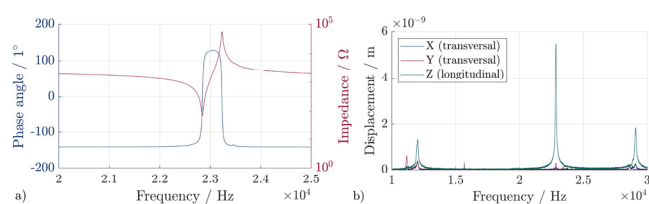


Fig. 3. Resonance behavior of the ultrasonic system
(a) Impedance and phase shift; (b) Frequency response in all three spatial directions.

Table 1. Experimental plan for out-of-process evaluations.

Parameter	Levels
Excitation	Noise / Chirp / Fixed frequency (11 frequencies)
Power	25% (150 V) / 50% (300 V) / 100% (570 V)

The first experiment was carried out to get a baseline regarding the noise behavior of the individual sensors. Afterwards the system was excited with a periodic chirp to see if the sensors produce the same results regarding the detection of the longitudinal resonance frequency as the impedance analysis and the analysis with the laser scanning vibrometer. A Fast Fourier Transform (FFT) was carried out for all sensor signals. The results are shown in Fig. 4 and Fig. 5. It can be seen that the sensors exhibit peaks at the determined resonance frequency at 22,579 Hz (fiber-optical sensor), 22,703 Hz (passive piezoelectric disk) and 22,886 Hz (accelerometer and strain gauges). The deviation of the values obtained with the accelerometer and strain gauges to the other sensors possibly result from the different resonance frequencies of the two sonotrodes. The variation of the value obtained from the passive piezoelectric disc might indicate a slightly different behavior of the piezoelectric stack of the transducer. One of the strain gauges showed aberrant behavior. The peak at the expected resonance frequency was small compared to the other calculated peaks at 7 kHz, 14 kHz and 22 kHz. A visual inspection of the affected strain sensor has shown that the bonding of the glue was insufficient and a delamination of the strain gauge has occurred at the edges and corners of the strain

gauge. It stands to reason that this causes a vibration of the strain gauge itself, which can be seen after FFT.

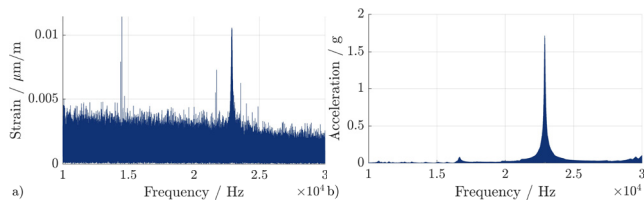


Fig. 4. Frequency response for Sonotrode 1
(a) Strain gauge 1; (b) Accelerometer.

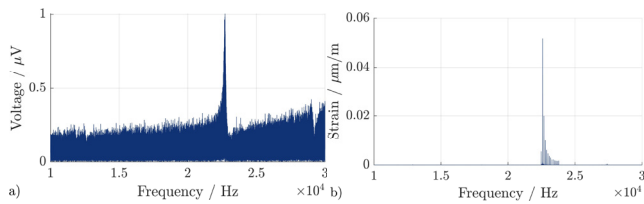


Fig. 5. Frequency response for Sonotrode 2
(a) Piezoelectric sensor disk; (b) Fiber-optical strain sensor.

The data of the experiments with a fixed frequency in the time domain gives a closer insight into the behavior of the sensors, see Fig. 6 and Fig. 7. Each figure shows a static state, when the generator is turned off, at the beginning and at the end of the measurement. Between these segments the generator was turned on. While the accelerometer constantly shows very high acceleration amplitudes in comparison to the noise, as seen in Fig. 6a, the strain gauges exhibit a worse signal-to-noise ratio (Fig. 6b). The passive piezoelectric disk exhibits even higher noise and additionally does not show a smooth behavior during operation, see Fig. 7a.

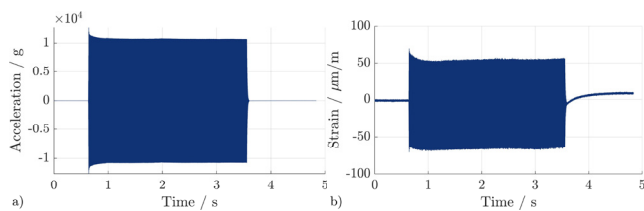


Fig. 6. Signals for Sonotrode 1 in the time domain
(a) Accelerometer; (b) Strain gauge 2.

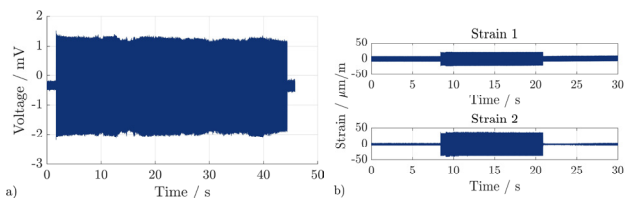


Fig. 7. Signals of Sonotrode 2 in the time domain
(a) Passive piezoelectric disk; (b) Fiber-optical sensors.

For the fiber-optical sensors both integrated fibers are analyzed. Firstly, it can be seen that both signals exhibit a high

strain amplitude during operation. Furthermore, Strain sensor 2 shows higher strain than Strain sensor 1, see Fig. 7b, which was to be expected as it is placed deeper in the sonotrode and therefore closer to the node, where strain is maximal. Additionally, upon closer inspection it can be seen that for both signals there is a quantization error. There is a discrepancy between the results gathered from the strain gauges and the fiber-optical sensors. The strain gauge shows strains of approximately 55 $\mu\text{m/m}$, while the fiber-optical strain sensors leads to values of approximately 20 $\mu\text{m/m}$ and 40 $\mu\text{m/m}$, respectively. This needs to be further investigated. Both figures show the signals gathered from controlling the system at the resonance frequency of 22,880 Hz with 100% power of the generator (570 V).

As shown, all of the sensors applied are in principle suited for measuring vibrations during the operation of the ultrasonic system. Consequently, they can be implemented in a turning process. The parameters and characteristics of the turning process are given in Table 2.

Table 2. Parameters and characteristics of the turning process.

Parameter / Characteristic	Value / Description
Material	Bronze (CuSn7Pb15-C)
Dimension	\varnothing 31 mm x 20 mm (diameter x length)
Tool	CCMW 060202 indexable inserts with special MCD tips
Clearance angle	25° (at tips)
Corner radius	0.09 mm (at tips)
Tool included angle	80°
Cutting edge angle	50°
Depth of cut a_p	0.1 mm
Frequency of the ultrasonic system	22,880 Hz
Direction of vibration	Radial
Cutting speed v_c	120 m/min / 480 m/min
Feed f	0.05 mm / 0.1 mm
Power of the generator	50% (300 V) / 100% (570 V)
Displacement amplitude (generator power level)	4.7 μm (50%) / 5.1 μm (100%)

Experimental investigations were realized on a precision lathe (PD 32, SPINNER Werkzeugmaschinen GmbH). Samples were premachined by external cylindrical turning to a diameter of 30.2 mm. Afterwards, turning experiments with an ultrasonic vibration superimposition were done. The experiments are carried out by a full factorial design of the parameters given in Table 2. Each combination was realized thrice, resulting in 24 single tests. Additionally, for each combination of cutting speed and feed, one sample was machined without ultrasonic vibration superimposition to get a baseline of the sensors during operation. The experiments were only done for Sonotrode 1 incorporating the accelerometer and the strain gauges. While machining, the whole system was mounted on a dynamometer to measure the components of the resultant force. During the assembly of the sonotrode with the

fiber-optical sensor the adhesive had soaked the coating of the fiber at the front end of the sonotrode and therefore the first segment of the coating became stiff. Because of this, the cable with the fiber could not be bent to a sufficiently small radius to avoid contact with the sample during machining.

4. Results and Discussion

The data gathered during the turning process shows the same behavior as for the preliminary investigations, see Fig. 8. Each graph visualizes a short period of time at the beginning of the measurement, when the system was stationary and there was no ultrasonic vibration. After this, the generator was turned on and the vibration becomes clearly visible in the data. Subsequently, machining was started. Depending on the combination of the cutting speed and the feed, the finishing process took between 2.36 s and 18.85 s.

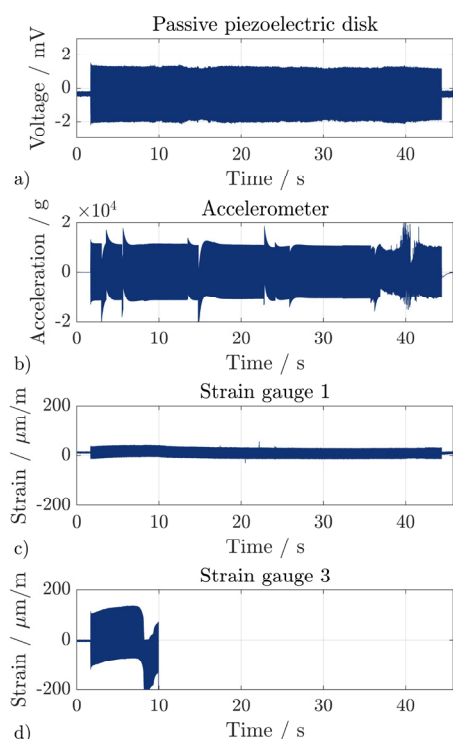


Fig. 8. Signal of the sensors in the time domain

(a) Passive piezoelectric disk; (b) Accelerometer; (c) Strain gauge 1 close to the front end of the sonotrode; (d) Strain gauge 3 close to the mount of the sonotrode.

There was no discernible difference in the gathered sensor signals before and during the machining. A possible explanation for this are the low cutting forces (highest component of the resultant force in all experiments) of approximately 3.8 N ($f = 0.05$ mm) or 5.9 N – 8.2 N ($f = 0.1$ mm), which are too small to affect the signals noticeably. The other components of the resultant force are generally smaller than 2 N. For higher components of the resultant forces, it is expected that there should be a peak in the time domain for the passive piezoelectric disk and the acceleration because of the contact of the tool and sample. For the strain

gauges a continuous offset during the turning process is expected because the whole sonotrode experiences a static compression (negative strain), as seen in [24]. The signal of the accelerometer shows erratic behavior at several points during operation, e.g. at 3 s, 3.5 s, 5.5 s etc. This might be attributed to the movement of the machine slide including the sonotrode and transducer, but the acceleration is too high for this. The reason for this is unclear as this was not reproducible during other tests. For this measurement the calculated vibration amplitude is approximately $5.28 \mu\text{m}$ at the front end of the sonotrode. Two strain gauges from different positions along the longitudinal axis of the sonotrode have been evaluated. Strain gauge 1 is placed close to the front end of the sonotrode, Strain gauge 3 near the flange. Therefore, Strain gauge 3 should experience higher strains as it is placed closer to the node of the sonotrode. This can be seen in Fig. 8d, but the signal for Strain gauge 3 ends at 10 s. This happened for strain gauges 4 – 6 as well. A visual inspection showed that the soldering joints of the electrical contacts became loose. The reason for this is probably the higher strain. This is supported by the fact that the contact separation only happened for the four strain gauges placed close to the node. The behavior of the sensors described above was the same for all measurements. There were no discernible differences in the time domain depending on the cutting speed or feed. At higher voltages (570 V / 100% of the generator) the behavior also did not change. This was apparent with all sensors. The reason for higher voltages not resulting in higher vibration amplitudes (strain, acceleration) may be that the energy is transformed into transversal vibrations, which could not be measured with the setup used, or even heat. Furthermore, during the measurements with higher voltages the sensor signals showed more occurrences of random peaks and higher noise during operation, which may be attributed to other excited frequencies. The expected frequencies resulting from the rotational speed of the main spindle of 21.22 Hz and 84.88 Hz was visible in the frequency domain of the passive piezoelectric disk and the strain gauges (not pictured). Fig. 9 shows a spectrogram for a turning process without (Fig. 9a) and one with ultrasonic vibration superimposition (Fig. 9b).

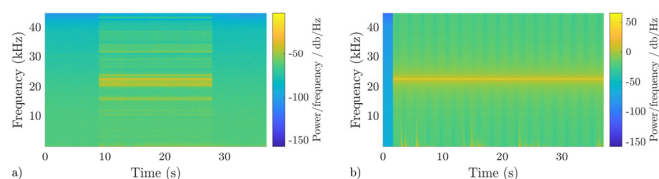


Fig. 9. Spectrogram of the accelerometer during turning (a) Without ultrasonic vibration superimposition; (b) With ultrasonic vibration superimposition.

For the turning process without ultrasonic vibration superimposition, it can be seen that there is an excitation of a broad frequency range during machining. It can be seen that the highest amplitudes occur at 22,880 Hz which corresponds with the resonance frequency of the ultrasonic system. This indicates that the system vibrates at its resonance frequency even without ultrasonic vibration superimposition. On the right

picture (Fig. 9b) the turning process is not visible, as the vibrations resulting from the process forces are not strong enough to be seen compared to the ultrasonic vibration.

5. Conclusion and outlook

This paper presents an approach for monitoring vibrations of an ultrasonic system during load-free oscillation and at a turning process. The sensors exhibit a high functionality in regard to their suitability for measuring vibrations at high frequencies. Strain sensors have in theory the potential to enable an in-process detection, but the application point has to be chosen carefully, so that they are not damaged during operation. The soldering points for four strain gauges have come loose and the vibration signals could therefore not be measured. The other strain gauges indicate no bending. The accelerometer shows the best signal-to-noise ratio and enables an in-process-calculation of the current displacement. This would benefit the manufacturing of microstructures significantly as it is of high importance to know the displacement of the tool precisely to produce a defined surface microstructure. Furthermore, the accelerometer is the only sensor, which shows a visible signal resulting from the turning process in the time domain. The passive piezoelectric disk placed at the piezoelectric stack in the transducer involves a sufficient signal-to-noise ratio and enables the detection of the resonance frequency, but lacks information regarding the vibration shape and displacement at the tool. Fiber-optical sensors integrated into the sonotrode show advantages, mainly in respect to detecting only longitudinal vibration modes, due to being placed along the neutral fiber and enabling a monitoring of the temperature during operation. However, their drawbacks consist in difficult cable routing and currently high noise in relation to the signal. For all sensors, higher process forces resulting from either larger areas of the undeformed chip or harder materials is necessary to achieve a higher external load and therefore mismatch between the operating frequency and the current resonance frequency of the ultrasonic system under load. Furthermore, the durability of the fixation of the sensors has to be investigated under constant operation as this proved to be insufficient for the strain gauges that experienced higher strain.

Acknowledgements

This research was funded by the Deutsche Forschungsgemeinschaft (DFG, German Research Foundation) – grant number 510749881.

References

- [1] Zheng WC, Huo D. Review of vibration devices for vibration-assisted machining. *The International Journal of Advanced Manufacturing Technology* 2020;108:1631-1651.
- [2] Yang C, Shan X, Xie T. Titanium wire drawing with longitudinal-torsional composite ultrasonic vibration. *The International Journal of Advanced Manufacturing Technology* 2016;83:645-655.
- [3] Michalski M. Grundlegende Untersuchungen zum Prozess- und Werkstoffverhalten bei schwingungsüberlagerter Umformung. FAU Studien aus dem Maschinenbau 2019.
- [4] Zhang C, Zhang J, Feng P. Mathematical model for cutting force in rotary ultrasonic face milling of brittle materials. *The International Journal of Advanced Manufacturing Technology* 2013;69:161–170.
- [5] Chang SSF, Bone GM. Burr size reduction in drilling by ultrasonic assistance. *Robotics and Computer-Integrated Manufacturing* 2005;21:442-450.
- [6] Singh R, Khamba JS. Mathematical modeling of tool wear rate in ultrasonic machining of titanium. *The International Journal of Advanced Manufacturing Technology* 2009;43:573-580.
- [7] Feucht F, Ketelaer J, Wolff A, Mori M, Fujishima M. Latest Machining Technologies of Hard-to-cut Materials by Ultrasonic Machine Tool. *Procedia CIRP* 2014;14:148-152.
- [8] Halim NFHA, Ascroft H, Barnes S. Analysis of Tool Wear, Cutting Force, Surface Roughness and Machining Temperature During Finishing Operation of Ultrasonic Assisted Milling (UAM) of Carbon Fibre Reinforced Plastic (CFRP). *Procedia Engineering* 2017;184:185-191.
- [9] Xu WX, Zhang LC. Ultrasonic vibration-assisted machining: principle, design and application. *Advances in Manufacturing* 2015;3:173-192.
- [10] Gallego-Juárez JA, Graff KF. *Power Ultrasonics: Applications of high-intensity ultrasound*. Amsterdam: Woodhead publishing; 2015.
- [11] Amini S, Khosrojerdi MR, Nosouhi, R. Elliptical ultrasonic-assisted turning tool with longitudinal and bending vibration mode. *Proceedings of the Institution of Mechanical Engineers, Part B: Journal of Engineering Manufacture* 2017;231:1389-1395.
- [12] Nad M. Ultrasonic horn design for ultrasonic machining technologies. *Applied and Computational Mechanics* 2015;4:79-88.
- [13] Shamoto E, Suzuki N, Moriwaki T, Naoi Y. Development of Ultrasonic Elliptical Vibration Controller for Elliptical Vibration Cutting. *CIRP Annals* 2002;51:327-330.
- [14] Zhang R, Steinert P, Schubert A. Microstructuring of Surface by Two-stage vibration-assisted Turning. *Procedia CIRP* 2014;14:136-141.
- [15] Schubert A, Nestler A, Pintermagel S, Zeidler H. Influence of ultrasonic vibration assistance on the surface integrity in turning of the aluminium alloy AA2017. *Materialwissenschaft und Werkstofftechnik* 2011;42:658-665.
- [16] Nestler A, Schubert A. Surface Properties in Ultrasonic Vibration Assisted Turning of Particle Reinforced Aluminium Matrix Composites. *Procedia CIRP* 2014;12:125-130.
- [17] Xu S, Kuriyagawa T, Shimada K, Mizutani M. Recent advances in ultrasonic-assisted machining for the fabrication of micro/nano-textured surfaces. *Frontiers of Mechanical Engineering* 2017;12:33-45.
- [18] Zhou H, Huang SH, Li W. Electrical Impedance Matching Between Piezoelectric Transducer and Power Amplifier. *IEEE Sensors Journal* 2020;20:14273-14281.
- [19] Yokozawa H, Twiefel J, Weinstein M, Morita T. Dynamic resonant frequency control of ultrasonic transducer for stabilizing resonant state in wide frequency band. *Japanese Journal of Applied Physics* 2017;56:07JE08.
- [20] Voronina S, Babitsky V. Autoresonant control strategies of loaded ultrasonic transducer for machining applications. *Journal of Sound and Vibration* 2008;313:395-417.
- [21] Li X, Meadows A, Babitsky V, Parkin R. Experimental analysis on autoresonant control of ultrasonically assisted drilling. *Mechatronics* 2015;29:57-66.
- [22] Werner JM, Engelmann M, Schmidt M, Titsch C, Dix M, Drossel WG. Comparison of Structural Integrated Piezoceramics, Piezoelectric Patches and Strain Gauges for Condition Monitoring. *Sensors* 2022;22:1-15.
- [23] Li X, Babitsky V, Parkin R, Meadows A. Autoresonant excitation and control of nonlinear mode for ultrasonically assisted drilling. *ZAMM Journal of Applied Mathematics and Mechanics* 2014;94:904-910.
- [24] Kimme S, Hafez N, Titsch C, Werner JM, Nestler A, Drossel WG. Close-to-process strain measurement in ultrasonic vibration-assisted turning. *Journal of Sensors and Sensor Systems* 2019;8:285-292.